Indian J. Pure Appl. Math., **45**(3): 321-341, June 2014
© Indian National Science Academy

EFFECT OF SUCTION/INJECTION ON FREE CONVECTION ALONG A VERTICAL PLATE IN A NANOFLUID SATURATED NON-DARCY POROUS MEDIUM WITH INTERNAL HEAT GENERATION

A. J. Chamkha*, A. M. Rashad**, Ch. Ram Reddy*** and P. V. S. N. Murthy****

**Manufacturing Engineering Department, Public Authority for Applied Education and Training, Shuweikh*, 70654 *Kuwait*

***Department of Mathematics, Aswan University*, *Faculty of Science*, 81528, *Egypt*

****Department of Mathematics, National Institute of Technology*, *Warangal* 506004, *India*

*****Department of Mathematics, Indian Institute of Technology*, *Kharagpur* 721302, *India*

e-mail: am_rashad@yahoo.com

(*Received* 4 *March* 2013; *after final revision* 20 *June* 2013; *accepted* 27 *August* 2013)

The effect of internal heat generation on free convection along a vertical plate embedded in a nanofluid saturated non-Darcy porous medium in the presence of suction/injection is analyzed. The non-linear governing equations and their associated boundary conditions are initially cast into dimensionless forms by non-dimensional variables. The resulting equations are solved numerically by an accurate, implicit, iterative finite-difference methodology and the obtained results are compared favorably with previously published work. A parametric study is performed to illustrate influence of the temperature exponent, non-Darcy, suction/injection, Brownian motion and thermophoresis parameters on the profiles of the velocity components, temperature and nanoparticle volume fraction. The numerical data for the heat and nanoparticle mass transfer rates have been tabulated for various parametric conditions.

Key words : Free convection; non-Darcy porous medium; nanofluid; suction/injection; internal heat generation.

1. INTRODUCTION

The study of convective flow, heat and mass transfer in porous media has been an active field of research as it plays a crucial role in diverse applications, such as thermal insulation, extraction of crude oil and chemical catalytic reactors, etc. Considerable work has been reported on flow, heat and mass transfer in Darcian porous media. Cheng and Minkowycz [1] presented similarity solutions for free convective heat transfer from a vertical plate in a fluid-saturated porous medium. The problem of combined convection from vertical plates in porous media is analyzed by Minkowycz *et al.* [2]. However, Darcy's law is valid only for slow flows through porous media with low permeability. At higher flow rates, there is a departure from the linear law and inertial effects become important. The simultaneous effects of fluid inertia force and boundary viscous resistance on the flow and heat transfer in a porous medium are discussed by Vafai and Tien [3] for forced convection and by Ranganathan and Viskanta [4] for mixed convection. From their reports, it is found that both boundary and inertia effects exhibit a significant influence on the velocity distribution and heat transfer and thus, these effects cannot be ignored. The Darcy-Forchheimer model describes the effect of inertia as well as viscous forces in porous media. A detailed review of convective heat transfer in Darcian and Non-Darcian porous medium can be found in the book by Nield and Bejan [5]. Several authors, Narayana and Murthy [6], Kairi and Murthy [7] and Chamkha *et al.* [8] to mention but few, have studied the convective heat and mass transfer over different surface geometries in a fluid saturated non-Darcy porous media.

A large number of physical phenomena involve free convection driven by internal heat generation. The most important applications are in the field of nuclear energy and also to fire and combustion modelling, the development of metal waste form from spent nuclear fuel and for storage of spent nuclear fuel. Studies in natural convection driven by internal heat generation have been done by Roberts [9], Jahn and Reinke [10], Hardee and Nilson [11], Stewart and Dona [12], etc. A couple of papers have been devoted to the subject of similarity solutions for free or mixed convection with internal heat generation in porous media for several geometric configurations, see Postelnicu *et al.* [13] and Chamkha [14]. For an exhaustive discussion of the free or mixed convection heat transfer in the boundary layers about different surface geometries in porous media in the presence of internal heat generation or absorption, the reader is referred to the works of Singh *et al.* [15] (also see the references cited therein).

The effect of blowing or suction on convective heat transfer over a vertical permeable sur-

face embedded in a porous medium has been the subject of several investigations. The problem has a number of important engineering and geophysical applications. For example, the residual warm water discharged from a geothermal power plan is usually disposed of through surface reinjection wells, which can be idealized as vertical plane sources in a porous medium (see Cheng [16]). If the temperature of the injected fluid differs from that of the receiving groundwater in the rock formations, injected fluid would experience a positive or negative buoyancy force, which results in a convective movement of groundwater near the wall. Cortell [17] investigated heat transfer in a porous medium over a stretching surface with internal heat generation and suction or injection. The effect of suction or injection on the free convection boundary layers induced by a heated vertical plate embedded in a saturated porous medium with an exponential decaying heat generation is studied by Ali [18]. Recently, Srinivasacharya *et al.* [19] presented a boundary layer analysis for mixed convection heat transfer in a non-Darcy saturated porous medium over a vertical plate with uniform wall temperature in the presence of suction/injection, magnetic and radiation effects.

In recent times, the flow analysis of nanofluids has been the topic of extensive research due to its characteristic in increasing thermal conductivity in heat transfer process. Several ordinary fluids including water, toluene, ethylene glycol and mineral oils etc. in heat transfer processes have rather low thermal conductivity. The nanofluid (initially introduced by Choi [20]) is an advance type of fluid containing nanometer sized particles (diameter less than 100 nm) or fibers suspended in the ordinary fluid. Undoubtedly, the nanofluids are advantageous in the sense that they are more stable and have acceptable viscosity and better wetting, spreading and dispersion properties on solid surface. Nanofluids are used in different engineering applications such as microelectronics, microfluidics, transportation, biomedical, solid-state lighting and manufacturing. The research on heat and mass transfer in nanofluids has been receiving increased attention worldwide. Many researchers have found unexpected thermal properties of nanofluids, and have proposed new mechanisms behind the enhanced thermal properties of nanofluids. Excellent reviews on convective transport in nanofluids have been made by Buongiorno [21] and Kakac and Pramuanjaroenkij [22]. The free convective boundary layer flows in a porous medium saturated by nanofluid have been analyzed by Nield and Kuznetsov ([23, 24]). They incorporated Brownian motion and thermophoresis effects. Also, it is interesting to note that the Brownian motion of nanoparticles at molecular and nanoscale levels are a key nanoscale mechanism governing their thermal behaviors. In nanofluid systems, due to the size of the

nanoparticles, the Brownian motion takes place, which can affect the heat transfer properties. As the particle size scale approaches to the nanometer scale, the particle Brownian motion and its effect on the surrounding liquids play an important role in the heat transfer. Chamkha *et al.* [25] presented a boundary layer analysis for the natural convection past an isothermal sphere in a Darcy porous medium saturated with a nanofluid. Nield and Kuznetsov [26] investigated the cross-diffusion in nanofluids, with the aim of making a detailed comparison with regular cross diffusion effects and the cross-diffusion effects peculiar to nanofluids, and at the same time investigating the interaction between these effects when the base fluid of the nanofluid is itself a binary fluid such as salty water. Recently, a boundary layer analysis for the natural convection past a horizontal plate in a porous medium saturated with a nanofluid is studied by Gorla and Chamkha [27]. But, very little attention has been paid to study the significance of combined effects of internal heat generation and suction/injection on free convection in a nanofluid saturated non-Darcy porous medium. Mahdy and Ahmed [28] performed numerical analysis to examine laminar free convective of a nanofluid along a vertical wavy surface saturated porous medium. Recently, the problem of natural convection from a vertical permeable cone in nanofluid saturated porous media for uniform heat and nanoparticles volume fraction fluxes has been investigated numerically Chamkha and Rashad [29]. These nanofluids appear to have a very high thermal conductivity and may be able to meet the rising demand as an efficient heat transfer agent. Scientists and engineers have started showing interest in the study heat transfer characteristics of these nanofluids. But a clear picture about the heat transfer through these nanofluids is yet to emerge.

The effect of suction/injection on free convection along a vertical plate in a nanofluid saturated non-Darcy porous medium in the presence of internal heat generation has not been reported in the literature. The aim of this investigation is to consider the combined effects of internal heat generation and suction/injection on the free convection along a vertical plate in a nanofluid saturated non-Darcy porous medium. The implicit, iterative finite-difference method discussed by Blottner [30] is employed to solve the nonlinear system of this particular problem. The effects of suction/injection, non-Darcy, internal heat generation parameters are examined and are displayed through graphs. The results are compared with relevant results in the existing literature and are found to be in good agreement.

2. MATHEMATICAL FORMULATION

Consider a vertical permeable flat plate of variable temperature $T_w(x) = T_\infty + Ax^\lambda$ and uniform nanoparticle concentration ϕ_w which is embedded in a steady laminar two-dimensional nanofluid saturated non-Darcy porous medium of constant ambient temperature T_∞ and nanoparticle concentration ϕ_∞. The values of T_w and ϕ_w are assumed to be greater than the ambient temperature T_∞ and concentration ϕ_∞ at any arbitrary reference point in the medium (inside the boundary layer). The coordinate system is chosen such that x-axis is along the vertical plate and y-axis normal to the plate. The physical model and the coordinate system are shown in Fig. 1. The porous medium is considered to be homogeneous and isotropic (i.e., uniform with a constant porosity and permeability) and is saturated with a nanofluid which is in local thermodynamic equilibrium with the solid matrix. The fluid has constant properties except the density in the buoyancy term of the balance of momentum equation. The fluid flow is moderate, so the pressure drop is proportional to the linear combination of fluid velocity and the square of velocity (Forchhiemer flow model is considered). By employing Oberbeck-

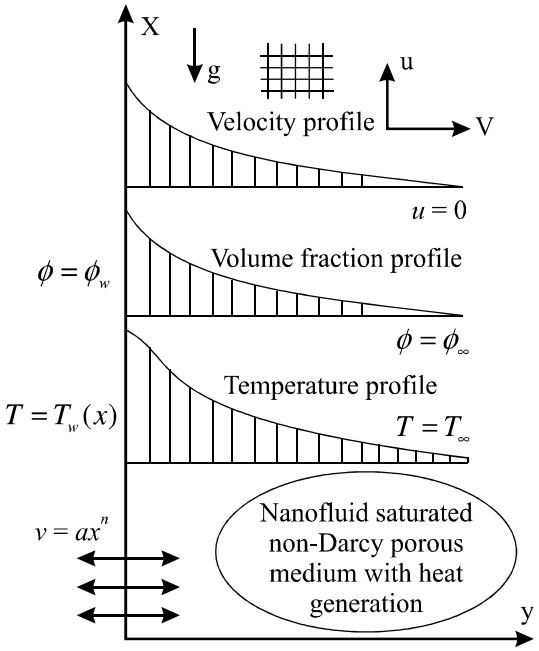

Figure 1: Physical model and coordinate system

Boussinesq approximation and making use of the standard boundary layer approximation and

the Darcy-Forchheimer model (Nield and Bejan [5]), the governing equations for the nanofluid are given by

$$\frac{\partial u}{\partial x} + \frac{\partial v}{\partial y} = 0 \tag{1}$$

$$u + \frac{c\sqrt{K}}{\left(\mu/\rho f_\infty\right)} u^2 = \frac{K\left(1-\phi_\infty\right)\,\rho f_\infty\, g\,\beta}{\mu}\,\left(T-T_\infty\right) - \frac{\left(\rho_p-\rho f_\infty\right)\,gK}{\mu}\,\left(\phi-\phi_\infty\right) \tag{2}$$

$$u\frac{\partial T}{\partial x} + v\frac{\partial T}{\partial y} = \alpha_m \frac{\partial^2 T}{\partial y^2} + J\left[D_B \frac{\partial \phi}{\partial y}\frac{\partial T}{\partial y} + \frac{D_T}{T_\infty}\left(\frac{\partial T}{\partial y}\right)^2\right] + \frac{q'''}{(\rho c)_f} \tag{3}$$

$$\frac{1}{\varphi}\left(u\frac{\partial \phi}{\partial x} + v\frac{\partial \phi}{\partial y}\right) = D_B\frac{\partial^2 \phi}{\partial y^2} + \frac{D_T}{T_\infty}\frac{\partial^2 T}{\partial y^2} \tag{4}$$

where *u* and *v* are the Darcy velocity components in *x* and *y* directions, respectively, *T* is the temperature, ϕ is the nanoparticle concentration, g is the acceleration due to gravity, *K* is the permeability, *c* is the empirical constant associated with the Forchheimer porous inertia term, φ is the porosity, $\alpha_m = k_m \Big/ (\rho c)_f$ is the thermal diffusivity of the fluid, $\nu = \mu/\rho f_\infty$ is the kinematic viscosity coefficient and $J = (\rho c)_p \Big/ (\rho c)_f$. Further, ρf_∞ is the density of the base fluid and $\rho,\ \mu,\ k_m$ and β are the density, viscosity, thermal conductivity and volumetric thermal expansion coefficient of the nanofluid, while ρ_p is the density of the nanoparticles, $(\rho c)_f$ is the heat capacity of the fluid and $(\rho c)_p$ is the effective heat capacity of the nanoparticle material. The coefficients that appear in Eqs. (3-4) are the Brownian diffusion coefficient D_B, the thermophoretic diffusion coefficient D_T and q''' is the internal heat generation. For, details of the derivation of Eqs. (1-4), one can refer the papers by Buongiorno [15] and Nield and Kuznetsov ([17], [19]).

The associated boundary conditions are

$$v = ax^n, \quad T = T_w(x) = T_\infty + Ax^\lambda, \quad \phi = \phi_w \quad \text{at} \quad y = 0 \tag{5}$$

$$u = 0, \quad T = T_\infty, \quad \phi = \phi_\infty \quad \text{as} \quad y \to \infty$$

where the subscripts *w* and ∞ indicate the conditions at the wall, and at the outer edge of the boundary layer, respectively. Further, A is positive constant, $a,\ n$ and λ are constants with $a > 0$ for injection, $a < 0$ for suction or withdrawal of fluid. In an attempt to find similarity

solutions for the governing equations (1-4) subject to the boundary conditions (5), we shall take $n = (\lambda - 1)/2$.

Introducing, the following non-dimensional transformations

$$\eta = \frac{y}{x} Ra_x^{\frac{1}{2}}, \;\; \psi(\eta) = \alpha_m Ra_x^{\frac{1}{2}} f(\eta), \;\; \theta(\eta) = \frac{T - T_\infty}{T_w - T_\infty}, \;\; S(\eta) = \frac{\phi - \phi_\infty}{\phi_w - \phi_\infty} \tag{6}$$

where α_m is the effective thermal diffusivity of the porous medium, and Ra_x is the local Rayleigh number, which is defined as

$$Ra_x = \frac{(1 - \phi_\infty)\, g\, K\, \beta\, (T_w - T_\infty)\, x}{\nu \alpha_m}.$$

We also assume that the heat generation q''' is given by

$$q''' = Q_0 \, \frac{k_m (T_w - T_\infty)}{x^2} Ra_x \; e^{-\eta} \tag{7}$$

where Q_0 is the heat generation(source)/absorption(sink) constant and has value $Q_0 = 0$, $Q_0 = -1$ or $Q_0 = 1$ for absence, heat absorption (sink) or heat generation (source), respectively.

In view of the continuity Eq. (1), we introduce the stream function ψ by

$$u = \frac{\partial \psi}{\partial y}, v = -\frac{\partial \psi}{\partial x} \tag{8}$$

Substituting Eq. (8) in Eqs. (2)-(4) and then using the non-dimensional transformations (6), we get the following system of non-dimensional equations:

$$f' + Gr\, f'^2 = \;\; \theta - \mathrm{N}r.\; S \tag{9}$$

$$\theta'' \; - \lambda\, f'\, \theta + \left(\frac{\lambda + 1}{2}\right) \;\; f\theta' + Nb.\, \theta'\, S' \; + \; Nt.\, \theta'^2 \; + Q_0 \; e^{-\eta} = 0 \tag{10}$$

$$S'' \; + \frac{1}{2}\, Le.f\, S' + \frac{Nt}{Nb} \; \theta'' = 0 \tag{11}$$

where the primes indicate partial differentiation with respect to η alone, $Gr = \dfrac{c\sqrt{K}}{\nu} \, \dfrac{\alpha_m}{x} \, Ra_x$ is the non-Darcy parameter, $Nr = \dfrac{(\rho_p - \rho f_\infty)(\phi_w - \phi_\infty)}{\rho f_\infty \beta (1 - \phi_\infty)(T_w - T_\infty)}$ is the buoyancy parameter, $Nb = \dfrac{J\, D_B (\phi_w - \phi_\infty)}{\alpha_m}$ is the Brownian motion parameter, $Nt = \dfrac{J\, D_T}{\alpha_m T_\infty} A\, x^\lambda$ is the thermophoresis parameter and $Le = \dfrac{\alpha_m}{\varphi\, D_B}$is the Lewis number.

The boundary conditions (5) in terms of $f,\ \theta$ and S become

$$\eta = 0: \quad f(0) = -f_w, \ \ \theta(0) = 1, \ \ S(0) = 1 \tag{12a}$$

$$\eta \to \infty: \quad f'(\infty) \to 0, \quad \theta(\infty) \to 0, \quad S(\infty) \to 0 \tag{12b}$$

where $f_w = \dfrac{2a}{(\lambda+1)\,\alpha_m}\left[\dfrac{\alpha_m \nu}{AKg\beta}\right]^{\frac{1}{2}}$ is the dimensionless injection or suction parameter. In particular, the plate is impermeable with $f_w = 0$ whereas the plate is permeable with injection or suction according to $f_w > 0$ or $f_w < 0$.

The local heat and local nanoparticle mass fluxes from the vertical plate can be obtained from

$$q_w = -k_m \left(\frac{\partial T}{\partial y}\right)_{y=0}, \qquad q_m = -D_B \left(\frac{\partial \phi}{\partial y}\right)_{y=0} \tag{13}$$

The dimensionless local Nusselt number $Nu_x = \dfrac{q_w\, x}{k_m\ (T_w - T_\infty)}$ and local nanoparticle Sherwood number $Sh_x = \dfrac{q_m\, x}{D_B\ (\phi_w - \phi_\infty)}$ are given by

$$\frac{Nu_x}{Ra_x^{\frac{1}{2}}} = -\theta'(0) \qquad \text{and} \qquad \frac{Sh_x}{Ra_x^{\frac{1}{2}}} = -S'(0) \tag{14}$$

The effects of the various parameters involved in this investigation on these coefficients are discussed in the Results and Discussion section.

3. NUMERICAL METHOD

The reduced flow governing equations (9)-(11) are non-linear, coupled, ordinary differential equations, which possess no closed-form solution. Therefore, they must be solved numerically subject to the boundary conditions given by Eq. (12). The implicit, iterative finite-difference method discussed by Blottner [30] has proven to be adequate for the solution of this type of equations. For this reason, this method is employed in the present work. Eqs. (9)-(11) are discretized using three-point central difference quotients. This converts the differential equations into linear sets of algebraic equations, which can be readily solved by the well known Thomas algorithm (see Blottner [30]). On the other hand, Eqs. (9)-(11) is discretized and solved subject to the appropriate boundary conditions by the trapezoidal rule. The computational domain in

the η-direction was made up of 196 non-uniform grid points. It is expected that most changes in the dependent variables occur in the region close to the plate where viscous effects dominate. However, small changes in the dependent variables are expected far away from the plate surface. For these reasons, variable step sizes in the η-direction are employed. The initial step size $\Delta\eta_1$ and the growth factor K^* employed such that $\Delta\eta_{i+1} = K^*\Delta\eta_i$ (where the subscript *i* indicates the grid location) were 10^{-3} and 1.0375, respectively. These values were found (by performing many numerical experimentations) to give accurate and grid-independent solutions. The solution convergence criterion employed in the present work was based on the difference between the values of the dependent variables at the current and the previous iterations. When this difference reached 10^{-5}, the solution was assumed converged and the iteration process was terminated.

The case of the free convection flow of Newtonian fluids along a vertical flat plate of Cheng [31] can be obtained by taking $Nr = 0$, $Gr = 0$, $Nb = 0$, $Nt = 0$, $Le = 0$ and $Q_0 = 0$ (i.e., in the absence of internal heat generation) and $S(\eta) \to 0$ (i.e., in the absence of nanofluid). Thus, in the absence of internal generation and nanofluid with $Nr = 0$, $Gr = 0$, $Nb = 0$, $Nt = 0$, $Le = 0$ the results of the governing equations (1)-(4) have been compared with the special case of (Cheng [31]) and it is found that they are in good agreement, as shown in Table 1. Therefore, the developed code can be used with great confidence to study the problem considered in this paper.

4. Results and Discussion

We have computed the solutions for the dimensionless velocity, temperature and nanoparticle volume fraction functions as shown graphically in Figs. 2(a)-8(c). The effects of suction or injection f_w, non-Darcy parameter Gr, Brownian motion parameter Nb, thermophoresis parameter Nt, Lewis number Le, buoyancy ratio Nr and internal heat generation have been discussed.

In Figs. 2(a)-2(c), the effect of the temperature exponent λ on the dimensionless velocity, temperature and the nanoparticle volume fraction profiles are presented for fixed values of Gr, Nr, Nb, Nt, f_w and Le. The case of $\lambda = 0$ corresponds to the uniform surface temperature, $\lambda = 1/3$ corresponds to the uniform surface heat flux and $\lambda = 1$ corresponds to the uniform wall temperature distribution. It can be observed from Fig. 2(a) that the maximum velocity

Table 1: Comparison of $-\theta'(0)$ for free convection along a vertical flat plate in Newtonian fluids (Cheng [31])

f_w	Cheng [31]			Present		
	$\lambda = 0$	$\lambda = 1/3$	$\lambda = 1$	$\lambda = 0$	$\lambda = 1/3$	$\lambda = 1$
1.0	0.2043	0.3971	0.6180	0.2046	0.3973	0.6188
0.8	0.2432	0.4416	0.6770	0.2435	0.4423	0.6775
0.6	0.2865	0.4917	0.7440	0.2869	0.4924	0.7448
0.4	0.3345	0.5476	0.8198	0.3346	0.5482	0.8202
0.2	0.3870	0.6096	0.9049	0.3869	0.6104	0.9057
0.0	0.4438	0.6776	1.0000	0.4441	0.6782	1.0012
-0.2	0.5050	0.7517	1.1040	0.5055	0.7520	1.1060
-0.4	0.5701	0.8316	1.2190	0.5706	0.8324	1.2207
-0.6	0.6389	0.9169	1.3440	0.6394	0.9185	1.3450
-0.8	0.7111	1.0070	1.4770	0.7121	1.0081	1.4781
-1.0	0.7863	1.1020	1.6180	0.7874	1.1040	1.6191

decreases as λ increases. From Fig. 2(b), we see that the temperature boundary layer thickness decreases with the increase of λ. This can physically be explained because the internal heat generation results in an increase in the buoyancy forces, which in turn reduce more flow along the plate. It can be seen from Fig. 2(c) that the nanoparticle volume fraction boundary layer thickness of the fluid increases with the increase of λ. Furthermore, the velocity and temperature of the nanofluid with uniform surface temperature distribution is more compared to the case of nanofluid with uniform surface heat flux distribution and then with uniform wall temperature distribution. An exactly reverse trend can be noticed in the case of nanoparticle volume fraction.

The dimensionless velocity distribution for different values of Forchheimer number *Gr* with the fixed values of λ,Nr, Nb, Nt, f_w and Le is depicted in Fig. 3(a). Since *Gr* represents the inertial drag, thus an increase in the Forchheimer number increases the resistance to the flow and so, a decrease in the fluid velocity ensues. Here, *Gr = 0* represents the case where the flow is Darcian. The velocity is maximum in this case due to the total absence of inertial drag. The dimensionless temperature for different values of Forchheimer number *Gr* for the fixed values of λ, Nr, Nb, Nt, f_w and Le, is displayed in Fig. 3(b). An increase in Forchheimer number *Gr*, increase temperature values, since as the fluid is decelerated, energy is dissipated as heat

is dissipated as heat and serves to increase temperatures. As such the temperature is minimized for the lowest value of *Gr* and maximized for the highest value of *Gr* as shown in Fig. 3(b). Fig. 3(c) demonstrates the dimensionless nanoparticle volume fraction for different values of Forchheimer number with the fixed values of λ, Nr, Nb, Nt, f_w and Le. As the Forchheimer number increases, the nanoparticle volume fraction boundary layer thickness increases. The increase in the non-Darcy parameter reduces the intensity of the flow but enhances the thermal and nanoparticle volume fraction boundary layer thicknesses.

The dimensionless velocity component for different values of the nanofluid buoyancy ratio *Nr* with fixed values of other parameters is depicted in Fig. 4(a). An increase in *Nr* is seen to considerably lower the momentum boundary layer thickness closer to the wall. Fig. 4(b) demonstrates the dimensionless temperature for different values of nanofluid buoyancy ratio *Nr*. A rise in the temperature boundary layer thickness is seen with increasing values of the *Nr*. Fig. 4(c) depicts that the dimensionless volume fraction for different values of nanofluid buoyancy ratio *Nr* for fixed values of other parameters. As the parameter *Nr* increases, the volume fraction profile increases for the specified conditions.

Figures (5) and (6) are prepared to present the effects of the Brownian motion *Nb* and thermophoresis *Nt* on the velocity, temperature and volume fraction distributions. With *Nb = 0*, there is no thermal transport due to buoyancy effects created as a result of nanoparticle concentration gradients. It is observed that the momentum boundary layer thickness increases with the increase of *Nb* and *Nt*. As the parameters *Nt* and *Nb* increase, the temperature increases but the nanoparticle volume fraction decreases for the specified conditions. As expected, the boundary layer profile for the temperature function is essentially the same form as in the case of a regular (Newtonian) fluid. The nanoparticle volume fraction decreases with an increase in *Nb* as well as with *Nt*. It is noticed that the nanoparticle volume fraction increases with an increase in *Nb* in the case of forced convection flow. We notice that, positive *Nt* indicates a cold surface while negative *Nt* corresponds to a hot surface. For hot surfaces, thermophoresis tends to blow the nanoparticle volume fraction boundary layer away from the surface since a hot surface repels the sub-micron sized particles from it, thereby forming a relatively particle-free layer near the surface.

Figures 7(a)-7(c) show the non-dimensional velocity, temperature and the volume fraction profiles for various values of the Lewis number *Le* for a given Gr, Nr, Nb, Nt, f_w and λ. It

is noticed from Fig. (7) that an increase in the Lewis number *Le* results in an increase in the velocity but decreases in the temperature and volume fraction within the boundary layer. This is because an increase in *Le* yields a decrease in diffusion which finally results into a decrease of volume fraction. Hence, the present analysis shows that the flow field is appreciably influenced by the Lewis number *Le*.

The effect of the suction/injection parameter $f_w$on the non-dimensional velocity, temperature and nanoparticle volume fraction distributions inside the boundary layer is shown in Fig. 8 with the fixed value of *Le,* $Gr,\ Nr,\ Nb$, Nt and λ for both the cases of injection (i.e., $f_w > 0$) and suction (*i.e,*$f_w < 0$). Moreover, injection (i.e., $f_w > 0$) of fluid adds up extra force which enhances the flow resulting in a larger molecular movement. This finally results into an increase in the volume fractions. It is evident from Fig. (8) that the fluid velocity, temperature and the volume fractions are more in the case of injection compared to the suction. It is also noted that the velocity, temperature and the volume fractions of the nanofluid in the absence of suction/injection are more compared to the case of a nanofluid with suction but less compared to the case of a nanofluid with injection.

The effects of various physical parameters on the Nusselt number and the nanoparticle Sherwood number are depicted in Tables 2 and 3. From these tables, it is seen that as the temperature exponent λ increases, there is a rise in the heat transfer rate but a fall in the nanoparticle mass transfer rate. The effect of the non-Darcy parameter *Gr* on the non-dimensional heat and nanoparticle mass transfer rates for fixed values of other parameters is presented in Table 2. It can be observed that, the heat transfer and nanoparticle mass transfer rates decrease with the increase in the values of *Gr*. Hence, the non-Darcy parameter has an important role in controlling the flow field. The similar trend can be found for the case of the nanoparticle buoyancy ratio *Nr*. Also it is found that as the Brownian motion parameter *Nb* increases, the heat transfer rate decreases, whereas the nanoparticle mass transfer rate decreases. Similar observations can be seen from this table with the increasing values of both *Nt* and *Le* for fixed values of other parameters. It is also noticed that an increase in the suction/injection parameter f_w leads to a fall in both the heat and nanoparticle mass transfer rates. Finally, it can be seen that the heat and nanoparticle mass transfer rates are more in the case of a nanofluid with suction whereas the heat and nanoparticle mass transfer rates are less in the case of a nanofluid with injection compared to the case of a nanofluid without suction/injection.

Table 2: Local Nusselt number Nu_x, and local nanoparticle Sherwood number Sh_x for different values of parametric study of the physical parameters with internal heat generation for $Nt = 0.1$, $Nb = 0.3$ and $Le = 10$

λ	Gr	Nr	f_w	$-\theta'(0)$	$-S'(0)$
0.0	1.0	0.1	0.0	-0.3436179	1.502032
1/3	1.0	0.1	0.0	-0.1021305	1.431334
1/2	1.0	0.1	0.0	-0.0105249	1.402081
1.0	1.0	0.1	0.0	0.2061414	1.325700
1.0	0.0	0.1	0.0	0.3961986	1.587130
1.0	1.0	0.1	0.0	0.2061414	1.325700
1.0	2.0	0.1	0.0	0.1173702	1.215727
1.0	3.0	0.1	0.0	0.0633131	1.150615
1.0	1.0	0.1	0.0	0.2061414	1.325700
1.0	1.0	0.3	0.0	0.1649567	1.259219
1.0	1.0	0.5	0.0	0.1170364	1.184118
1.0	1.0	0.7	0.0	0.0590220	1.095151
1.0	1.0	0.1	-0.5	0.3712308	3.172052
1.0	1.0	0.1	-0.3	0.2999960	2.377004
1.0	1.0	0.1	0.0	0.2061414	1.325700
1.0	1.0	0.1	0.3	0.1289631	0.5529845
1.0	1.0	0.1	0.5	0.0869758	0.2468835

Table 3: Local Nusselt number Nu_x, and local nanoparticle Sherwood number Sh_x for different values of parametric study of the physical parameters with $\lambda = 1$, $Gr = 0.1$, $Nr = 0.1$ and $f_w = 0$

Nb	Nt	Le	$-\theta'(0)$	$-S'(0$
0.1	0.1	10	0.2437131	1.314276
0.3	0.1	10	0.2061414	1.325700
0.5	0.1	10	0.1716965	1.330328
0.7	0.1	10	0.1411379	1.334241
0.3	0.1	10	0.2061414	1.325700
0.3	0.3	10	0.1895379	1.360727
0.3	0.5	10	0.1747626	1.406208
0.3	0.7	10	0.1607664	1.461310
0.3	0.1	1.0	0.2203662	0.3063079
0.3	0.1	10	0.2061414	1.325700
0.3	0.1	100	0.2056825	4.316015
0.3	0.1	1000	0.2091098	13.68964

5. CONCLUSIONS

In this paper, the effects of internal heat generation, suction/injection on free convection in a non-Darcy porous medium saturated with nanofluid in the presence of uniform variable wall temperature and uniform nanoparticle volume fraction were studied. Using the dimensionless variables, the governing equations were transformed into a set of non-linear parabolic equations where a numerical solution was presented using the implicit, iterative finite difference method discussed by Blottner [30] for a wide range of parameters. The following conclusions were obtained:

1. Increasing the value of the temperature exponent λ resulted in lower velocity, temperature distributions and nanoparticle mass transfer rate but higher nanoparticle volume fraction distribution and heat transfer rate in the boundary layer.

2. An increase in the non-Darcy parameter *Gr* resulted in decreases in the velocity distribution, heat and nanoparticle mass transfer rates and increases in the temperature and nanoparticle volume fraction distributions.

3. An increase in the Brownian motion parameter *Nb*, enhanced the velocity and temperature distributions and nanoparticle mass transfer rate but reduced the nanoparticle volume fraction and heat transfer rate in the boundary layer.

4. An increase in the thermophoresis parameter *Nt* caused decreases in the velocity, temperature, nanoparticle volume fraction distributions and the non-dimensional heat transfer rate but an increase in the nanoparticle mass transfer rate in the boundary layer.

5. An increase in the Lewis number *Le* produced reductions in the temperature and nanoparticle volume fraction distributions and heat transfer rate and increases in the velocity disctribution and nanoparticle mass transfer rate in the boundary layer.

6. An increase in the suction/injection parameter f_w resulted in enhancements in the velocity, temperature and the nanoparticle volume fraction distributions and reductions in the non-dimensional heat and nanoparticle mass transfer rates in the boundary layer.

7. An increase in the nanoparticle buoyancy parameter *Nr* produced reductions in the velocity distribution, heat and nanoparticle mass transfer rates and increases in the temperature and nanoparticle volume fraction distributions.

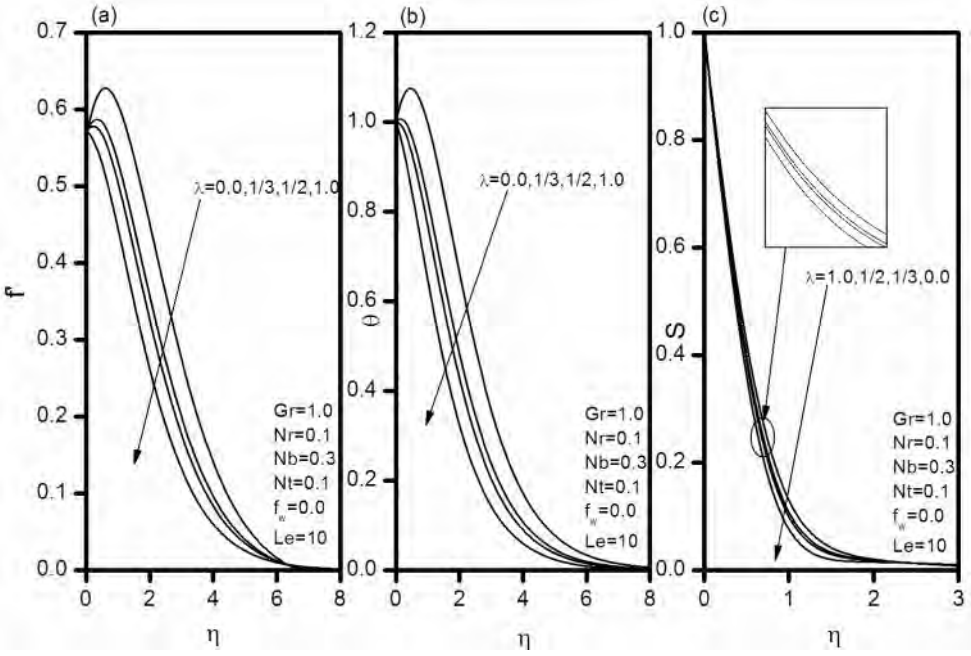

Figure 2: Effect of temperature exponent on (a) velocity, (b) temperature, and (c) volume fraction

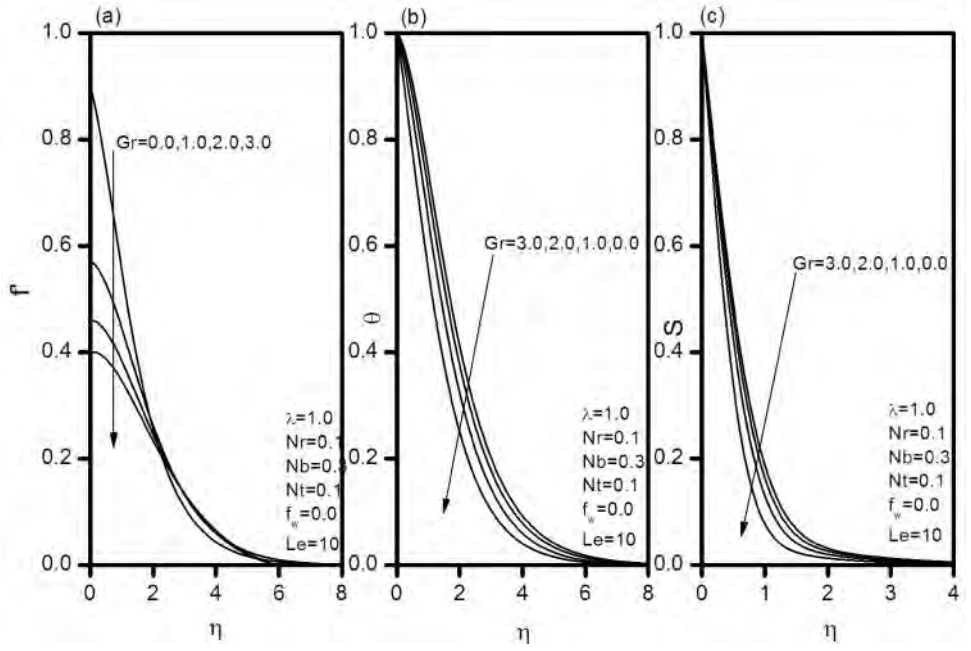

Figure 3: Effect of non-Darcy parameter on (a) velocity, (b) temperature, and (c) volume fraction

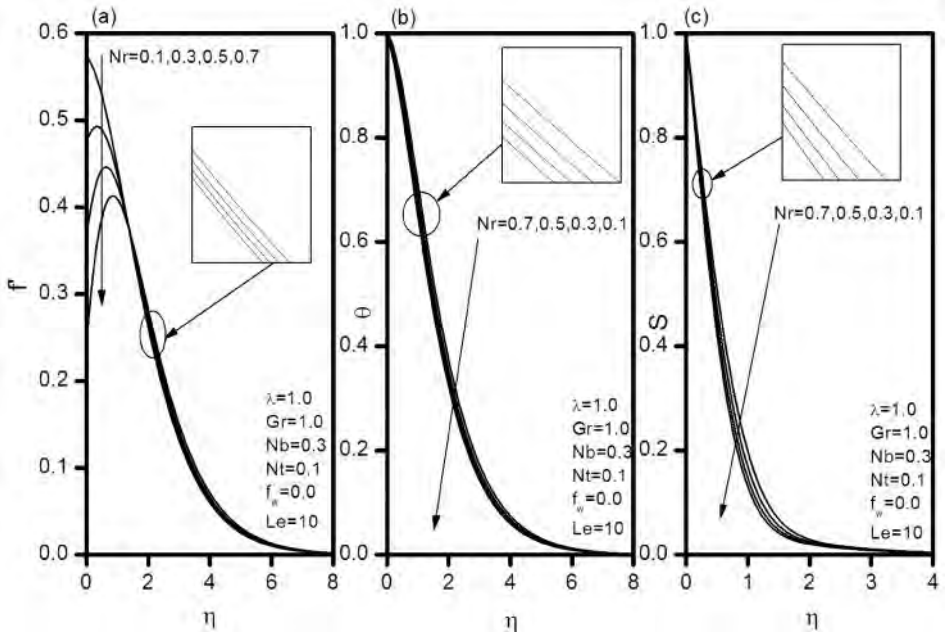

Figure 4: Effect of buoyancy parameter on (a) velocity, (b) temperature, and (c) volume fraction

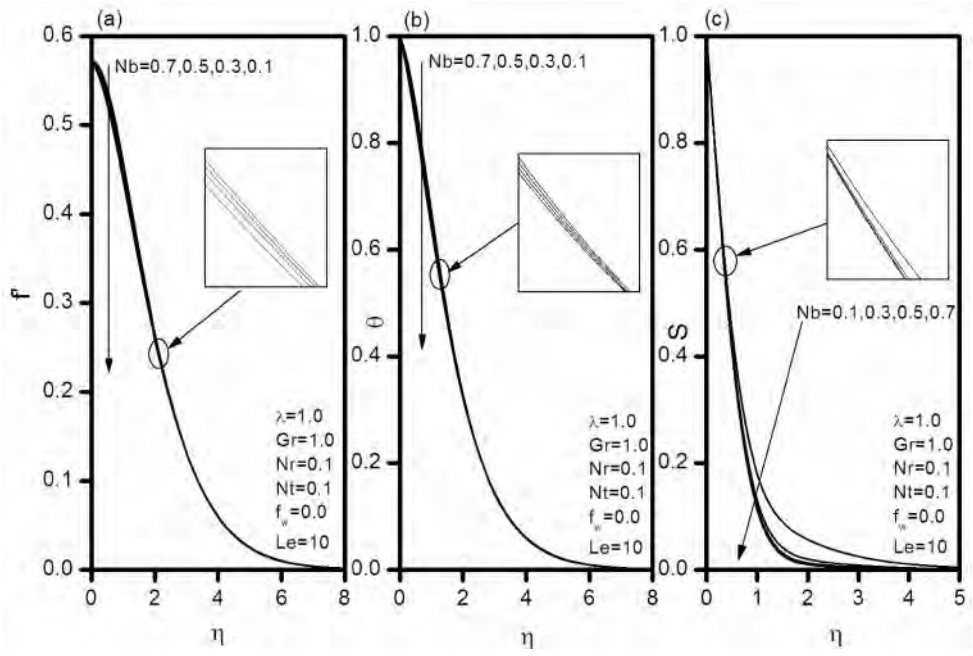

Figure 5: Effect of Brownian motion parameter on (a) velocity, (b) temperature, and (c) volume fraction

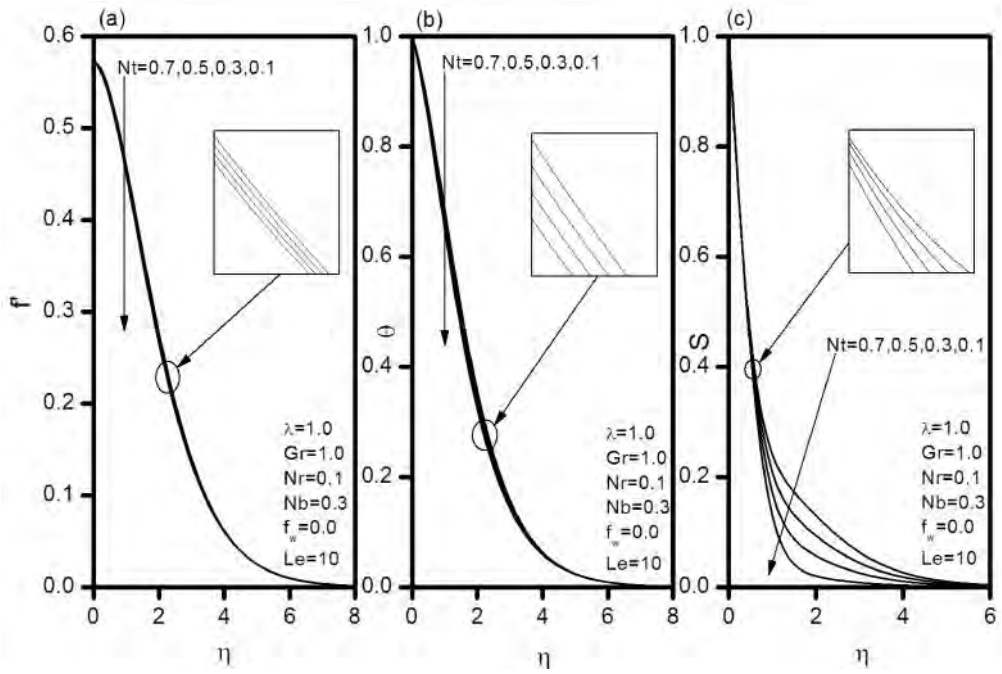

Figure 6: Effect of thermophoresis parameter on (a) velocity, (b) temperature, and (c) volume fraction

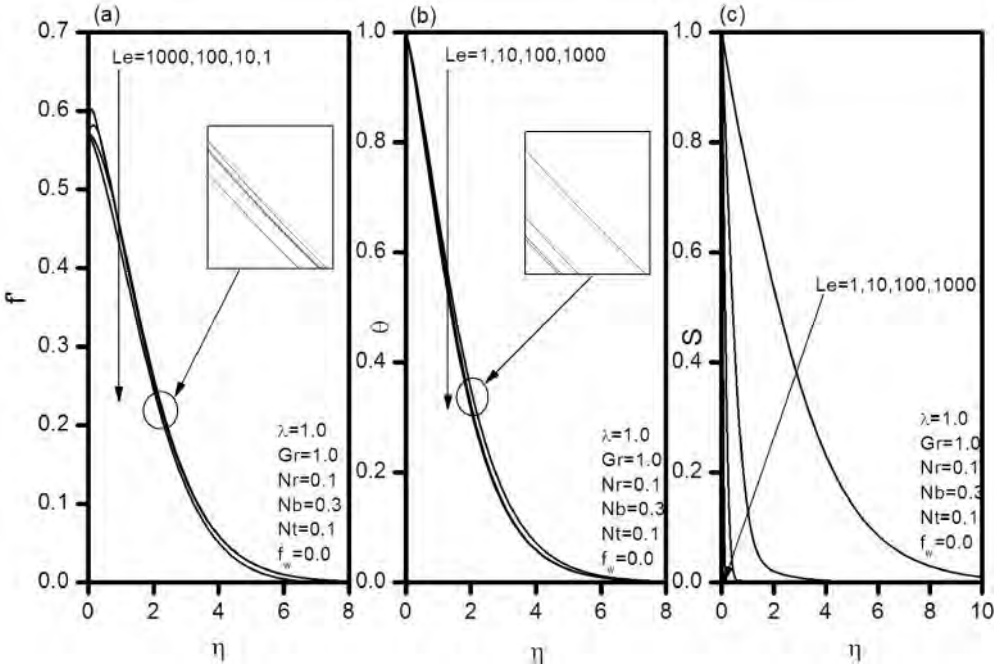

Figure 7: Effect of Lewis number on (a) velocity, (b) temperature, and (c) volume fraction

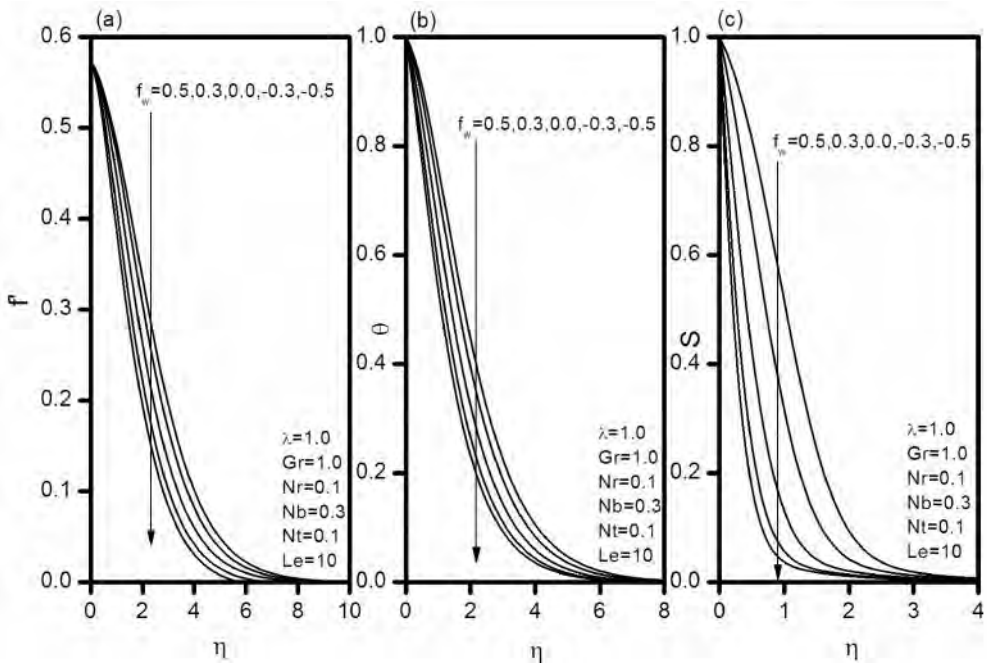

Figure 8: Effect of suction/injection on (a) velocity, (b) temperature, and (c) volume fraction

8. The results also indicated that the presence of internal heat generation, suction/injection in a nanofluid saturated non-Darcy porous medium influenced the flow, heat and nanoparticle volume fraction of the fluid flow.

9. It is also concluded from the results that as the nanoparticle buoyancy parameter *Nr* increased from 0.1 to 0.7, the rate of heat transfer decreased sufficiently by 249 % and the rate of mass transfer increased by 21%. Moreover, as the Brownian motion parameter *Nb* raised from 0.1 to 0.7, the rate of heat transfer reduced by 73 % while the rate of mass transfer enhanced slightly by 1%. Finally, as the thermophoresis parameter *Nt* increased from 0.1 to 0.7, the rate of heat transfer decreased by 28 % while the rate of mass transfer increased by 9%.

REFERENCES

1. P. Cheng and W. J. Minkowycz, Free convection about a verticalflat plate embedded in a saturated porous medium with applications to heat transfer, *Dike. J. Geophys. Res.*, **82** (1977), 2040-2044.

2. P. Cheng, *Natural Convection in a Porous Medium: Natural Convection: Fundamentals and Applications,* Hemisphere Publishers, Washington, DC., (1985), 475-513.

3. K. Vafai and C.L. Tien, Boundary and inertia effects on flow and heat transfer in porous media, *Int. J Heat Mass Transfer*, **24** (1981), 195-203.

4. P. Ranganathan and R. Viskanta, Mixed convection boundary layer flow along a vertical surface in a porous medium, *Numer. Heat Transfer*, **7** (1984), 305-317.

5. D. A. Nield and A. Bejan, *Convection in Porous Media*, 3rd edn. Springer-Verlag, New-York (2006).

6. P. A. L. Narayana and P. V. S. N. Murthy, Free convective heat and mass transfer in a doubly stratified non-Darcy porous medium, *J. Heat Transfer*, **128** (2006), 1204-1212.

7. R. R. Kairi and P. V. S. N. Murthy, Free convection in a thermally stratified non-Darcy porous medium, *Int. J. of Fluid Mechanics Research*, **36** (2009), 414-423.

8. A. J. Chamkha, S. M. M. EL-Kabeir and A. M. Rashad, Heat and mass transfer by non-Darcy free convection from a vertical cylinder embedded in porous media with a temperature-dependent viscosity, *Int. J. of Numerical Methods for Heat & Fluid Flow*, **21** (2011), 847-863.

9. P. H. Roberts, Convection in horizontal layers with internal heat generation: theory, *J. Fluid Mech.*, **30** (1967), 33-49.

10. M. Jahn and H. H. Reinke, Free convection heat transfer with internal energies sources: calculation and measurements, Paper NC 2.8, *Proceedings of the 5th Int. Heat Transfer Conference, Tokyo, Japan*, (1974), 74-78.

11. H. C. Hardee and P. H. Nilson, Natural convection in porous media with heat generation, *Nuclear Sci. Engng*, **63** (1977), 119-132.

12. W. E. Stewart and C. L. G. Dona, Free convection in a heat-generating porous medium in a finite vertical cylinder, *ASME Journal of Heat Transfer*, **110** (1988), 517-520.

13. A. Postelnicu, I. Pop and D. Grosan, Free convection boundary-layer flows over a vertical permeable flat plate in porous media with internal heat generation, *Int. Comm. Heat Mass Transfer*, **27** (2000), 729-738.

14. A. J. Chamkha, A. F. Al-Mudhaf and I. Pop, Effect of heat generation or absorption on thermophoretic free convection boundary layer from a vertical flat plate embedded in a porous medium, *Int. Commun Heat and Mass Transfer*, **33** (2006), 1096-1102.

15. G. Singh, P. R. Sharma and A. J. Chamkha, Effect of volumetric heat generation/absorption on mixed convection stagnation point flow on an iso-thermal vertical plate in porous media, *Int. J. Industrial Mathematics,* **2** (2010), 59-71.

16. P. Cheng, The influence of lateral mass flux on free convection boundary layers in a saturated porous medium, *Int. J. Heat Mass Transfer*, **20** (1977), 201-206.

17. R. Cortell, Flow and heat transfer of a fluid through a porous medium over a stretching surface with internal heat generation/absorption and suction/blowing, *Fluid Dynamics Research*, **37** (2005), 231-245.

18. M. E. Ali, The effect of lateral mass flux on the natural convection boundary layers induced by a heated vertical plate embedded in a saturated porous medium with internal heat generation, *Int. J. of Thermal Sciences*, **46** (2007), 157-163.

19. D. Srinivasacharya, J. Pranitha and Ch. RamReddy, MHD and Radiation effects on non-Darcy mixed convection, *Int. J. of Nonlinear Science*, **10** (2010), 61-69.

20. S. U. S. Choi, *Enhancing thermal conductivity of fluid with nanoparticles*, D.A. Siginer, H.P.Wang (Eds.), Developments and Applications of Non-Newtonian Flows, FED-V. 231/MD-V. 66, ASME, New York, (1995), 99-105.

21. J. Buongiorno, Convective transport in nanofluids, *ASME J Heat Transfer*, **128** (2006), 240-250.

22. S. Kakac and A. Pramuanjaroenkij, Review of convective heat transfer enhancement with nanofluids, *Int. J. Heat Mass Transfer*, **52** (2009), 3187-3196.

23. D. A. Nield and A. V. Kuznetsov, The Cheng-Minkowycz problem for natural convective boundary-layer flow in a porous medium saturated by a nanofluid, *Int. J. of Heat and Mass Transfer*, **52** (2009a), 5792-5795.

24. D. A. Nield and A. V. Kuznetsov, Thermal instability in a porous medium layer saturated by a nanofluid, *Int. J. Heat Mass Transfer*, **52** (2009b), 5796-5801.

25. A. J. Chamkha, R. S. R. Gorla and K. Ghodeswar, Non-similar solution for natural convective boundary layer flow over a sphere embedded in a porous medium saturated with a nanofluid, *Transp Porous Med.*, **86** (2011), 13-22.

26. D. A. Nield and A. V. Kuznetsov, The Cheng-Minkowycz problem for the double-diffusive natural convective boundary layer flow in a porous medium saturated by a nanofluid, *Int. J. of Heat and Mass Transfer*, **54** (2011), 374-378.

27. R. S. R. Gorla and A. J. Chamkha, Natural convective boundary layer flow over a horizontal plate embedded in a porous medium saturated with a nanofluid, *Journal of Modern Physics*, **2** (2011), 62-71.

28. A. Mahdy and S. E. Ahmed, Laminar free convection over a vertical wavy surface embedded in a porous medium saturated with a nanofluid, *Transp Porous Med.*, **91** (2012), 423-435.

29. A. J. Chamkha and A. M. Rashad, Natural Convection from a vertical permeable cone in nanofluid saturated porous media for uniform heat and nanoparticles volume fraction fluxes, *Int. J. of Numerical Methods for Heat and Fluid Flow*, **22** (2012), 1073-1085.

30. F. G. Blottner, Finite-difference methods of solution of the boundary layer equations, *AIAA J.*, **8** (1970), 193-205.

31. P. Cheng, The influence of lateral mass flux on free convection boundary layers in a saturated porous medium, *Int. J. Heat Mass Transfer*, **20** (1977), 201-206.